Unconventional Rydberg pumping and applications in quantum information processing

D. X. Li and X. Q. Shao*

Center for Quantum Sciences and School of Physics, Northeast Normal University, Changchun 130024, People's Republic of China and Center for Advanced Optoelectronic Functional Materials Research, and Key Laboratory for UV Light-Emitting Materials and Technology of Ministry of Education, Northeast Normal University, Changchun 130024, China

(Received 3 June 2018; published 28 December 2018)

We propose a mechanism of unconventional Rydberg pumping (URP) via simultaneously driving each Rydberg atom by two classical fields with different strengths of Rabi frequencies. This mechanism differs from the general Rydberg blockade or Rydberg antiblockade since it is closely related to the ground states of atoms, i.e., two atoms in the same ground state are stable while two atoms in different ground states are resonantly excited. Furthermore, we find the URP can be employed to simplify some special quantum information processing tasks, such as implementation of a three-qubit controlled-PHASE gate with only a single Rabi oscillation, preparation of two- and three-dimensional steady-state entanglement with two identical atoms, and realization of the autonomous quantum error correction in a Rydberg-atom-cavity system. The feasibility of the above applications is discussed explicitly by the state-of-the-art technology.

DOI: 10.1103/PhysRevA.98.062338

I. INTRODUCTION

The features of the interatomic Rydberg interactions open many possibilities to explore neutral atoms in the research of few- and many-body physics and quantum information applications [1]. One of the critical effects is the Rydberg blockade: In a small volume, once a Rydberg atom is excited to the Rydberg state, the strong, long-range interactions between Rydberg atoms will significantly suppress the excitation of other Rydberg atoms. After the first scheme to perform fast gate operations by the Rydberg blockade was proposed by Jaksch *et al.* [2], a variety of proposals were designed theoretically and experimentally for quantum computation [3–9], entanglement generation [10–15], quantum algorithms [16], quantum simulators [17], and quantum repeaters [18]. Another dramatic effect making use of the interatomic Rydberg interactions is the Rydberg dressing, which results from the adiabatical dressing between the ground state and the excited Rydberg state [19–21]. It enables tunable, anisotropic interactions and provides the possibility to study the novel exotic many-body physics [22–26]

In addition, the combination of interatomic Rydberg interactions and two-photon detuning leads to an opposite effect, the Rydberg antiblockade, which was theoretically predicted by Ates *et al.* [27] and was experimentally observed by Amthor *et al.* [28]. The Rydberg antiblockade can achieve the simultaneous excitations of two Rydberg atoms and can restrain the Rydberg blockade. The corresponding exploration is of particular interest, not only for two-qubit or multiqubit logic gates [29–31], but also for preparations of quantum entanglement [32–37], e.g., Carr and Saffman analyzed an approach to obtain high-fidelity entanglement and antiferromagnetic states by Rydberg antiblockade [32]. Quite recently, our group made use of the cooperation between Rydberg antiblockade, quantum Zeno dynamics, and atomic spontaneous emission to prepare the tripartite Greenberger-Horne-Zeilinger (GHZ) state and W state, respectively [36,37]. Moreover, by virtue of the Rydberg-antiblockade effect and the Raman transition, we have devised a mechanism of ground-state blockade to generate high-fidelity entanglement [38].

In this paper, we propose an unconventional Rydberg pumping (URP) scheme, which is different from all the above effects. This effect is closely related to the ground states of atoms, i.e., two atoms in the same ground state are stable while two atoms in different ground states are resonantly excited. Taking the case of two atoms as an example, the corresponding atomic levels are shown in Fig. 1(a). Both atoms consist of two ground states $|0\rangle$ and $|1\rangle$, and one Rydberg state $|r\rangle$. For each atom, the Rydberg state is dispersively coupled with the ground state $|1\rangle$ via a classical field of Rabi frequency Ω_1, detuning $-\Delta$, and another classical field resonantly drives the transition $|1\rangle \leftrightarrow |r\rangle$ with Rabi frequency Ω_2. Exploiting the URP, we can freeze the evolution of state $|11\rangle$, and only the states $|10\rangle$ and $|01\rangle$ can be excited into $|r0\rangle$ and $|0r\rangle$, respectively. In contrast, it is impossible for the Rydberg blockade and Rydberg antiblockade to inhibit the transitions $|11\rangle \leftrightarrow (|1r\rangle + |r1\rangle)/\sqrt{2}$ or $|11\rangle \leftrightarrow |rr\rangle$ and realize $|10(01)\rangle \leftrightarrow |r0(0r)\rangle$ simultaneously. We will illustrate the mechanism in detail in the next section and discuss its applications in three-qubit controlled-PHASE gate, steady-state entanglement, and autonomous quantum error correction in succession.

The remainder of the paper is organized as follows: In Sec. II, we illustrate the mechanism of the URP in detail with two three-level atoms. In Sec. III, we apply the technique to achieve a three-qubit controlled-PHASE gate. In Sec. IV, we discuss the possibility to dissipatively prepare the two- and three-dimensional entangled states by the URP. In Sec. V, we

*Corresponding author: shaoxq644@nenu.edu.cn

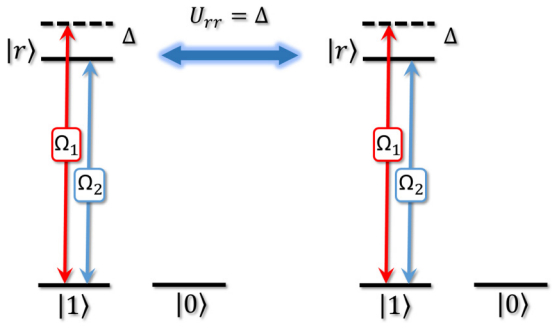

FIG. 1. Two-atomic-level configuration for the URP. The Rydberg state is dispersively coupled with the ground state $|1\rangle$ via a classical field of Rabi frequency Ω_1, detuning $-\Delta$, and another classical field resonantly driving the transition $|1\rangle \leftrightarrow |r\rangle$ with Rabi frequency Ω_2.

make use of the URP to realize the autonomous quantum error correction in a Rydberg-atom-cavity system. We summarize our works in Sec. VI.

II. MECHANISM OF THE URP BETWEEN TWO ATOMS

The effectiveness of the URP is not limited to the two-atom case, but it is instrumental enough for us to interpret the mechanism of the URP clearly with a bipartite system. The system includes two Λ-type three-level Rydberg atoms, which are shown in Fig. 1(a). The quantum information is encoded into the subspace $\{|00\rangle, |01\rangle, |10\rangle, |11\rangle\}$. In the interaction picture, the Hamiltonian of the system can be written as

$$H_I = \sum_{j=1}^{2} \Omega_1 e^{-i\Delta t} |r\rangle_{jj}\langle 1| + \Omega_2 |r\rangle_{jj}\langle 1| + \text{H.c.} + U_{rr}|rr\rangle\langle rr|, \quad (1)$$

where the subscript j means the jth atom and U_{rr} denotes the Rydberg-mediated interaction. After choosing $U_{rr} = \Delta$ (the condition will constrain the geometry of the atomic system because U_{rr} is dependent on the interatomic distance), we can utilize the formula $i\dot{U}_0^\dagger U_0 + U_0^\dagger H_I U_0$ to reformulate the Hamiltonian in a rotating frame with respect to $U_0 = \exp\{-itU_{rr}|rr\rangle\langle rr|\}$,

$$H_I = H_I^{(1)} + H_I^{(2)} + H_I^{(3)}, \quad (2)$$

where

$$H_I^{(1)} = \Omega_2(|r0\rangle\langle 10| + |0r\rangle\langle 01|) + \text{H.c.},$$
$$H_I^{(2)} = \sqrt{2}(\Omega_1|D\rangle\langle rr| + \Omega_2|D\rangle\langle 11|) + \text{H.c.},$$
$$H_I^{(3)} = \sqrt{2}e^{-i\Delta t}(\Omega_1|D\rangle\langle 11| + \Omega_2|D\rangle\langle rr|) + \Omega_1 e^{-i\Delta t}(|r0\rangle\langle 10| + |0r\rangle\langle 01|) + \text{H.c.},$$

and $|D\rangle = (|1r\rangle + |r1\rangle)/\sqrt{2}$. For the sake of clarity, according to Eq. (2) we show the corresponding diagram of collective two-atom energy levels and transitions in Fig. 2. The three ground states $|10\rangle$, $|11\rangle$, and $|01\rangle$ are pumped to the single excited states $|r0\rangle$, $|D\rangle$, and $|0r\rangle$, respectively. Furthermore, only the state $|D\rangle$ can be driven into the biexcitation state $|rr\rangle$, respectively. In the limit of $\Delta \gg \Omega_1 \gg \Omega_2$, $H_I^{(3)}$ can be

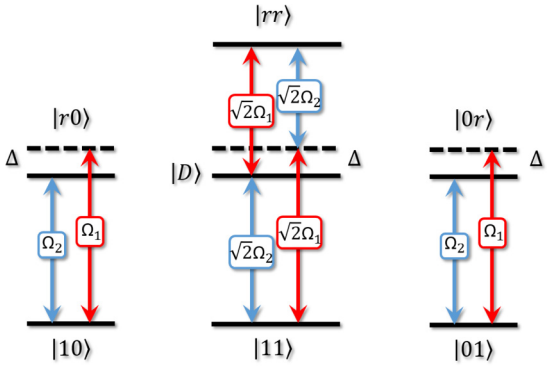

FIG. 2. The diagram of collective two-atom energy levels and transitions to illustrate Eq. (2).

reduced as the Stark-shift terms,

$$H_I^{(3)} = \frac{2\Omega_1^2}{\Delta}|11\rangle\langle 11| + \frac{\Omega_1^2}{\Delta}|10\rangle\langle 10| + \frac{\Omega_1^2}{\Delta}|01\rangle\langle 01| - \frac{\Omega_1^2}{\Delta}|r0\rangle\langle r0| - \frac{\Omega_1^2}{\Delta}|0r\rangle\langle 0r|, \quad (3)$$

and it can be further canceled out via introducing other ancillary levels. (Terms of $2\Omega_1\Omega_2|rr\rangle\langle 11|/\Delta + \text{H.c.} + 2\Omega_2^2|rr\rangle\langle rr|/\Delta$ have been ignored since $\Omega_1 \gg \Omega_2$.) Then we expand $H_I^{(2)}$ in terms of the basis of $\{|11\rangle, |+\rangle, |-\rangle\}$, where $|\pm\rangle = (|rr\rangle \pm |D\rangle)/\sqrt{2}$ are the eigenvectors of $\sqrt{2}\Omega_1|D\rangle\langle rr| + \text{H.c.}$ with respect to the eigenvalues $\pm\sqrt{2}\Omega_1$, i.e.,

$$H_I^{(2)} = \sqrt{2}\Omega_1(|+\rangle\langle +| - |-\rangle\langle -|) + \Omega_2(|+\rangle\langle 11| - |-\rangle\langle 11| + \text{H.c.}). \quad (4)$$

From the above equation, we can find that the effective form of $H_I^{(2)}$ is equal to 0 as $\Omega_1 \gg \Omega_2$. In other words, a quantum state initialized in $|11\rangle$ will not evolve into others, since the corresponding detunings are $\pm\sqrt{2}\Omega_1$. Therefore the Hamiltonian $H_I^{(2)}$ of Eq. (2) can be also neglected further. Finally, the total Hamiltonian has been simplified as

$$H_I \simeq H_{\text{eff}} = H_I^{(1)} = \Omega_2(|r0\rangle\langle 10| + |0r\rangle\langle 01|) + \text{H.c.}, \quad (5)$$

which signifies that in the limiting condition of URP, i.e., $U_{rr} = \Delta \gg \Omega_1 \gg \Omega_2$, the qubits system will not evolve except for the subspace spanned by $\{|01\rangle, |10\rangle\}$.

For explicitly determining the suitable values to satisfy the limiting condition of URP, we plot the evolutions of populations of states $|00\rangle$ (dash-dotted line), $|11\rangle$ (middle solid line), $|01\rangle$ (empty triangles), $|10\rangle$ (dashed line), $|0r\rangle$ (empty circles), $|r0\rangle$ (dotted line), $|r1\rangle$ (lower green solid line), $|1r\rangle$ (lower red solid line), and $|rr\rangle$ (lower black solid line) with different values of Δ/Ω_1 and Ω_1/Ω_2 in Fig. 3. We can find that the larger the values of Δ/Ω_1 and Ω_1/Ω_2, the more stable the states $\{|11\rangle, |1r\rangle, |r1\rangle, |rr\rangle\}$, and the more identical to the unitary evolution of Eq. (5) the behaviors of states $\{|10\rangle, |01\rangle, |r0\rangle, |0r\rangle\}$. Furthermore, $\Delta = 50\Omega_1$ and $\Omega_2 = 0.05\Omega_1$ are good enough to excellently execute the URP as shown in Fig. 3(d), where the states $\{|1r\rangle, |r1\rangle, |rr\rangle\}$ are almost vanished.

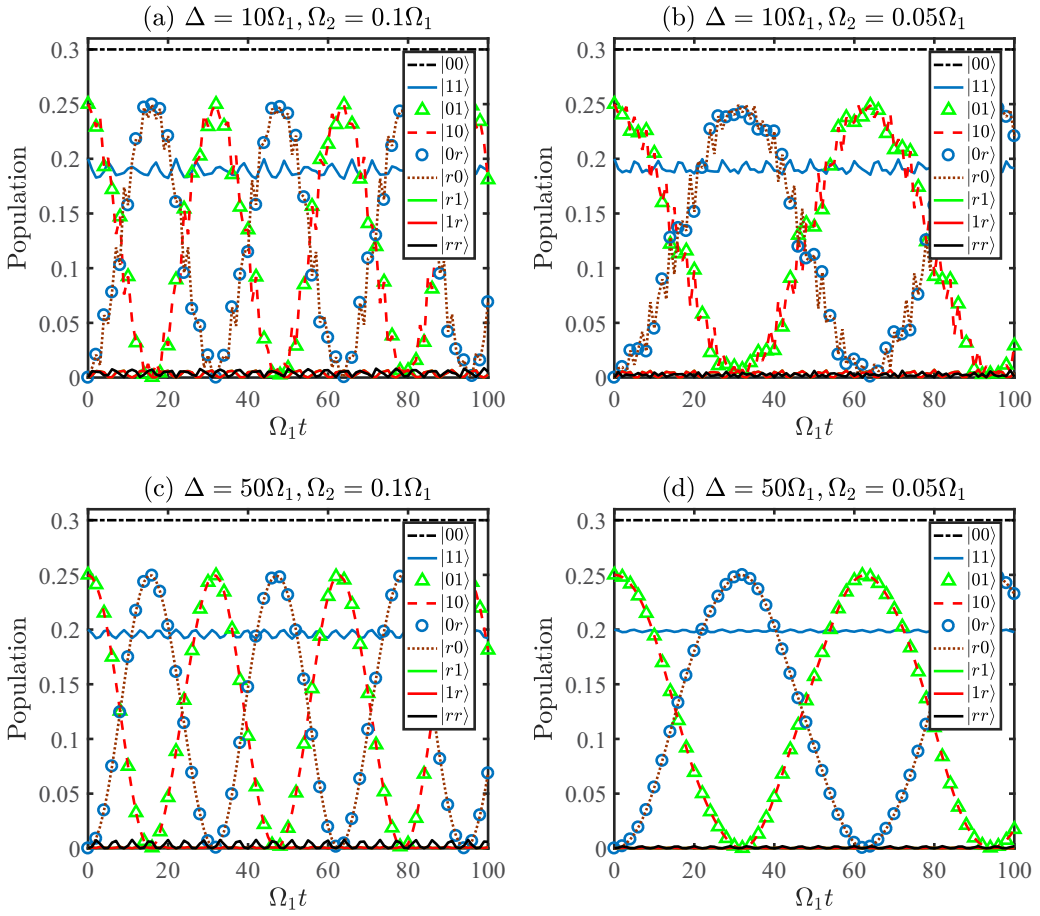

FIG. 3. The populations as functions of $\Omega_1 t$ governed by the Liouville equation $\dot{\rho}(t) = -i[H_I, \rho(t)]$ with different Δ/Ω_1 and Ω_1/Ω_2, where the population of state $|\psi\rangle$ is defined as $P = \langle\psi|\rho(t)|\psi\rangle$ and the initial states are all chosen as a random mixed state $\rho_0 = 0.2|11\rangle\langle 11| + 0.3|00\rangle\langle 00| + 0.25|10\rangle\langle 10| + 0.25|01\rangle\langle 01|$.

III. THREE-QUBIT CONTROLLED-PHASE GATE

It is universally acknowledged that the n-qubit controlled-PHASE gate is an essential ingredient for quantum algorithms [39–41] and quantum Fourier transform [42]. Here we implement a three-qubit controlled-PHASE gate by the URP, which can be finished with a single Rabi oscillation of a single atom in a short time. The atomic level of each atom remains the same as Fig. 1(a), and the Hamiltonian reads

$$H_I = \sum_{j=1}^{3} \Omega_1 e^{-i\Delta t}|r\rangle_{jj}\langle 1| + \Omega_2|r\rangle_{jj}\langle 1| + \text{H.c.} + \sum_{k>j} U_{rr}|rr\rangle_{jk}\langle rr|, \quad (6)$$

where we have considered that the interactions between different atoms are identical to U_{rr}. In the limiting condition $U_{rr} = \Delta \gg \Omega_1 \gg \Omega_2$, on the basis of the analysis in Sec. II, it is evident that the system initialized in $\{|000\rangle, |110\rangle, |101\rangle, |011\rangle\}$ will be stable. What makes the tripartite system different from the bipartite system is that for the system initialized in $|111\rangle$, the Rydberg antiblockade will result in an effective Hamiltonian $6\Omega_1^3(|111\rangle\langle rrr| + |rrr\rangle\langle 111|)/\Delta^2$. Although these terms are adverse for our purpose, they can be ignored because the contribution of $6\Omega_1^3/\Delta^2$ is much smaller than Ω_2 in the limiting condition $\Delta \gg \Omega_1$. Thus the total effective Hamiltonian of the three-qubit controlled gate can be written as

$$H_{\text{eff}} = \Omega_2(|r00\rangle\langle 100| + |0r0\rangle\langle 010| + |00r\rangle\langle 001|) + \text{H.c.} \quad (7)$$

In Fig. 4, we show the effective transitions of the three-qubit controlled-PHASE gate according to Eq. (7). In our system, only the states with one atom in $|1\rangle$

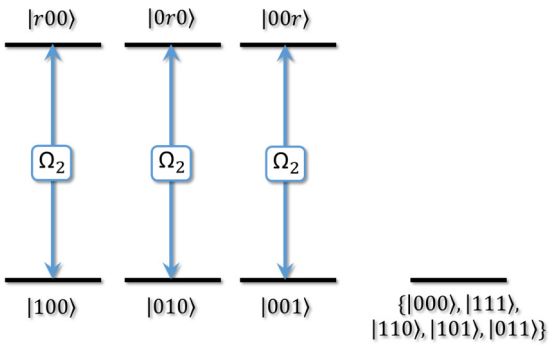

FIG. 4. The effective transitions of three-qubit controlled-PHASE gate. Only the states with one atom in $|1\rangle$ will undergo a Rabi oscillation with Rabi frequency Ω_2 while the other states are stable.

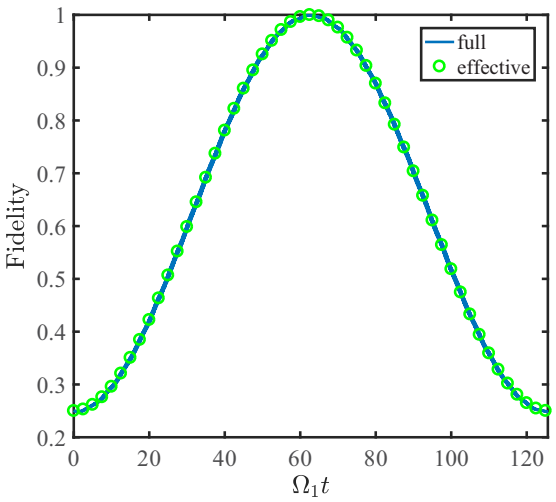

FIG. 5. The evolutions of corresponding fidelity governed by the H_I of Eq. (6) (solid line) and the H_{eff} of Eq. (7) (empty circles), respectively. The initial state is $|\psi_0\rangle$, and the parameters are chosen as $\Omega_2 = 0.05\Omega_1$ and $\Delta = 58\Omega_1$.

will undergo a Rabi oscillation with Rabi frequency Ω_2, while the other states are stable. Consequently, we carry out the three-qubit controlled-PHASE gate after the interaction time $T = \pi/\Omega_2$, which maps the direct product state of three atoms $|\psi_0\rangle = (|0\rangle + |1\rangle)_1(|0\rangle + |1\rangle)_2(|0\rangle + |1\rangle)_3/2\sqrt{2}$ into the three-atom entanglement $|\psi_s\rangle = (|000\rangle + |011\rangle + |101\rangle + |110\rangle + |111\rangle - |100\rangle - |010\rangle - |001\rangle)/2\sqrt{2}$. To demonstrate the feasibility of our scheme, we compare the evolutions of corresponding fidelity governed by H_I of Eq. (6) (solid line) and H_{eff} of Eq. (7) (empty circles) in Fig. 5, respectively. The fidelity is defined as $F = |\langle\psi_s| \exp(-i H_I t)|\psi_0\rangle|$. In Fig. 5, the two curves are in good agreement with each other and the corresponding fidelity can reach 99.94%, which adequately illuminates the validity of the effective system and the feasibility of the mechanism.

In experiment, the Rydberg atoms with a suitable principal quantum number can achieve the long radiative lifetimes [43], which can inhibit the detrimental effects of atom spontaneous emission for the three-qubit controlled-PHASE gate, e.g., the $97d_{5/2}$ Rydberg state with the decay rate $\gamma \simeq 2\pi \times 1$ kHz [44]. When we consider the Rydberg state $|r\rangle$ decays to the ground state with the same rate $\gamma/2 = 2\pi \times 1/2$ kHz, the decay of the jth atom can be described as Lindblad operators $L_j^{0(1)} = \sqrt{\gamma/2}|0(1)\rangle_{jj}\langle r|$ and the evolution of system will be governed by the master equation

$$\dot{\rho} = -i[H_I, \rho] + \mathcal{L}\rho, \tag{8}$$

where

$$\mathcal{L}\rho = \sum_{j=1}^{3}\sum_{k=0}^{1} L_j^k \rho L_j^{k\dagger} - \frac{1}{2}\left(L_j^{k\dagger} L_j^k \rho + \rho L_j^{k\dagger} L_j^k\right). \tag{9}$$

Meanwhile, the Rabi laser frequency Ω_1 and Ω_2 can be tuned continuously between $2\pi \times (0, 100)$ MHz in experiment [36,44]. Thus, the other parameters are set as

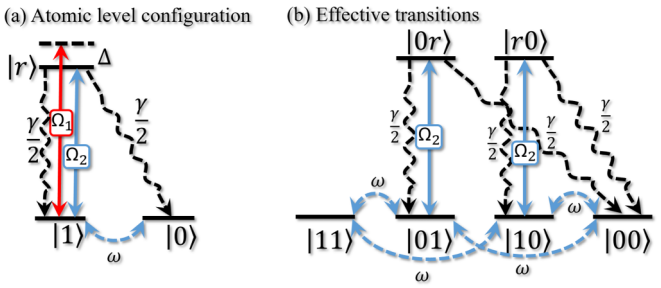

FIG. 6. (a) The atomic level configuration of the scheme to dissipatively prepare bipartite entanglement. (b) The corresponding effective transitions.

$(\Omega_1, \Omega_2, \Delta) = 2\pi \times (1, 0.05, 58)$ MHz and a high fidelity of $F = \sqrt{\langle\psi_s|\rho(\pi/\Omega_2)|\psi_s\rangle} = 99.37\%$ can be achieved.

IV. DISSIPATIVE GENERATION OF ENTANGLEMENT

A. Two-dimensional entangled state

With the rapid development of quantum information, more and more interest has been devoted to preparing quantum entanglement with the quantum noise, which can be regarded as a resource [45–47]. Combining the URP with the spontaneous emission of two Rydberg atoms, we propose a dissipative way to generate the Bell state $|\phi_-\rangle = (|00\rangle - |11\rangle)/\sqrt{2}$, which is independent of the initial state. As shown in Fig. 6(a), in addition to the classical fields driving the transitions between $|r\rangle$ and $|1\rangle$ dispersively and resonantly, we add the microwave fields to resonantly drive $|1\rangle \leftrightarrow |0\rangle$ with Rabi frequency ω. The branching ratios of spontaneous emission for the jth atom from $|r\rangle$ downwards to $|0\rangle$ and $|1\rangle$ are both assumed to be $\gamma/2$, described by the Lindblad operators $L_j^{0(1)} = \sqrt{\gamma/2}|0(1)\rangle_{jj}\langle r|$. The corresponding Hamiltonian and full master equation can be respectively indicated as

$$\begin{aligned} H_I &= H_L + H_{MW}, \\ H_L &= \sum_{j=1}^{2} \Omega_1 e^{-i\Delta t}|r\rangle_{jj}\langle 1| + \Omega_2|r\rangle_{jj}\langle 1| + \text{H.c.} \\ &\quad + U_{rr}|rr\rangle\langle rr|, \\ H_{MW} &= \sum_{i=1}^{2} \omega|1\rangle_{jj}\langle 0| + \text{H.c.}, \end{aligned} \tag{10}$$

and

$$\begin{aligned} \dot{\rho} &= -i[H_I, \rho] + \mathcal{L}\rho, \\ \mathcal{L}\rho &= \sum_{j=1}^{2}\sum_{k=0}^{1} L_j^k \rho L_j^{k\dagger} - \frac{1}{2}\left(L_j^{k\dagger} L_j^k \rho + \rho L_j^{k\dagger} L_j^k\right). \end{aligned} \tag{11}$$

According to the principle of the URP, H_L can be simplified as $H_L = \Omega_2(|01\rangle\langle 0r| + |10\rangle\langle r0|) + \text{H.c.}$ Then, expanding the H_{MW} with the basis of $\{|11\rangle, |01\rangle, |10\rangle, |00\rangle\}$, we can reformulate the Hamiltonian as follows:

$$\begin{aligned} H_{\text{eff}} &= \Omega_2(|10\rangle\langle r0| + |01\rangle\langle 0r|) + \omega(|11\rangle + |00\rangle) \\ &\quad \otimes(\langle 01| + \langle 10|) + \text{H.c.}, \end{aligned} \tag{12}$$

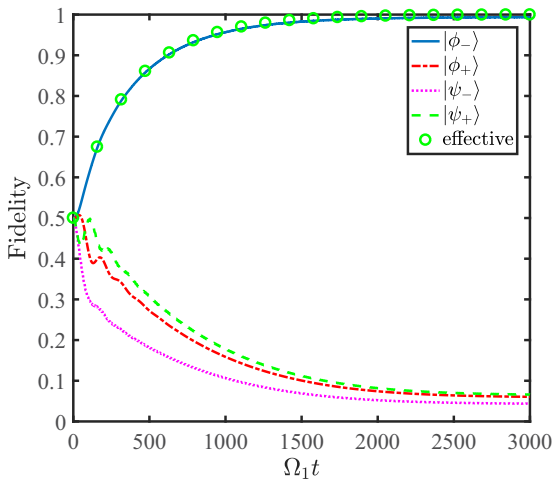

FIG. 7. The evolutions of fidelity for the Bell states governed by the full and effective master equations. The initial state is $\rho_0 = 0.25|00\rangle\langle 00| + 0.25|10\rangle\langle 10| + 0.25|01\rangle\langle 01| + 0.25|11\rangle\langle 11|$. The relevant parameters are chosen as $\Omega_2 = 0.02\Omega_1$, $\omega = 0.01\Omega_1$, $\Delta = 100\Omega_1$, and $\gamma = 0.05\Omega_1$.

with the corresponding effective master equation,

$$\dot{\rho} = -i[H_{\text{eff}}, \rho] + \mathcal{L}_{\text{eff}}\rho,$$
$$\mathcal{L}_{\text{eff}}\rho = \sum_{k=1}^{4} L_{\text{eff}}^{k}\rho L_{\text{eff}}^{k\dagger} - \frac{1}{2}\left(L_{\text{eff}}^{k\dagger}L_{\text{eff}}^{k}\rho + \rho L_{\text{eff}}^{k\dagger}L_{\text{eff}}^{k}\right), \quad (13)$$

where

$$L_{\text{eff}}^{1} = \sqrt{\frac{\gamma}{2}}|01\rangle\langle 0r|, \quad L_{\text{eff}}^{2} = \sqrt{\frac{\gamma}{2}}|00\rangle\langle 0r|,$$
$$L_{\text{eff}}^{3} = \sqrt{\frac{\gamma}{2}}|10\rangle\langle r0|, \quad L_{\text{eff}}^{4} = \sqrt{\frac{\gamma}{2}}|00\rangle\langle r0|.$$

In Fig. 6(b), we illustrate the effective transitions to intuitively explain the operational principle. The interconversion between four ground states $|11\rangle$, $|01\rangle$, $|10\rangle$ and $|00\rangle$ is realized by the microwave fields, and the ground states $|10\rangle$ and $|01\rangle$ are also coupled with the excited states $|r0\rangle$ and $|0r\rangle$, which will then spontaneously decay to the ground states $|01\rangle$, $|10\rangle$ and $|00\rangle$. The total transitions construct a cyclic evolution of system, and we can find that the Bell state $|\phi_-\rangle$ is the unique steady-state solution of Eq. (13) because of $H_{\text{eff}}|\phi_-\rangle = L_{\text{eff}}^{k}|\phi_-\rangle = 0$. Therefore, the system will be stabilized at the state $|\phi_-\rangle$ ultimately.

In Fig. 7, we compare the time evolutions of the fidelity for the target state $|\phi_-\rangle$ governed by the full master equation (solid line) and the effective master equation (empty circles) to confirm the validity of the above derivations. The tendencies of the two curves are identical, which implies that the reduced system is accurate and we can forecast the behavior of the realistic system by the reduced system. On the other hand, we find that the fidelity of the target state can arrive at 99.35% and the fidelities of states $|\phi_+\rangle = (|00\rangle + |11\rangle)/\sqrt{2}$ (dash-dotted line), $|\psi_+\rangle = (|01\rangle + |10\rangle)/\sqrt{2}$ (dashed line), and $|\psi_-\rangle = (|01\rangle - |10\rangle)/\sqrt{2}$ (dotted line) all tend to vanish, which demonstrates the behavior of the dissipative scheme. When we choose the experimental parameters as $(\Omega_1, \Omega_2, \omega, \Delta, \gamma) = 2\pi \times (1, 0.02, 0.01, 100, 0.03)$ MHz [48], the fidelity of the target state can be above 99.48%.

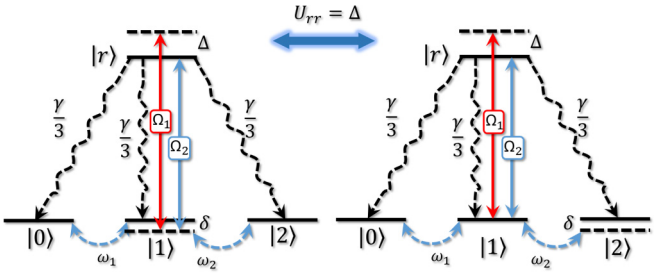

FIG. 8. The atomic level configuration of the scheme to prepare the three-dimensional entangled state with dissipation.

B. Three-dimensional entangled state

As is well known, the high-dimensional entanglement can not only violate the local realism more strongly than the two-dimensional entanglement [49], but also enhance the security of quantum key distribution [50,51]. Compared with the previous methods to generate the three-dimensional entanglement, such as those of Refs. [33] and [46], we can acquire the three-dimensional entanglement with two identical atoms and fewer driving fields. Once we adjust the dissipative scheme of two-dimensional entanglement slightly, the three-dimensional entanglement $|T_1\rangle = (|00\rangle - |11\rangle + |22\rangle)/\sqrt{3}$ can be prepared via URP and atomic spontaneous emission without a specific initial state.

The scheme of three-dimensional entanglement includes two four-level Rydberg atoms, both consisting of three ground states $|0\rangle$, $|1\rangle$, $|2\rangle$ and one Rydberg state $|r\rangle$, which has been plotted in Fig. 8. For the first Rydberg atom, the ground state $|1\rangle$ is driven to the Rydberg state $|r\rangle$ by two independent laser fields with Rabi frequencies Ω_1 and Ω_2, detuning $-\Delta - \delta$ and $-\delta$, respectively. Meanwhile, it is coupled with the other ground states $|0\rangle$ and $|2\rangle$ with a resonant microwave field (Rabi frequency ω_1) and a dispersive microwave field (Rabi frequency ω_2, detuning $-\delta$), respectively. For the second Rydberg atom, the transition $|1\rangle \leftrightarrow |r\rangle$ is achieved by a dispersive laser field with Rabi frequencies Ω_1, detuning $-\Delta$, and a resonant laser field with Rabi frequencies Ω_2, respectively. The transitions between ground states $|0\rangle \leftrightarrow |1\rangle$ and $|1\rangle \leftrightarrow |2\rangle$ are resonantly and dispersively coupled by two microwave fields with Rabi frequencies ω_1 and ω_2, respectively. The detuning of the latter is δ. The Hamiltonian of the total system can be written as

$$H_I = H_R + H_{MW},$$
$$H_R = \sum_{j=1}^{2}(\Omega_1 e^{-i\Delta t} + \Omega_2)|r\rangle_{jj}\langle 1| + \text{H.c.} + U|rr\rangle\langle rr|,$$
$$H_{MW} = \sum_{j=1}^{2}\omega_1|1\rangle_{jj}\langle 0| + \omega_2|1\rangle_{jj}\langle 2| + \text{H.c.} + \delta(|0\rangle_{11}\langle 0| + |1\rangle_{11}\langle 1| + |2\rangle_{22}\langle 2|). \quad (14)$$

The atomic spontaneous emission of the jth atom can be described as $L_j^0 = \sqrt{\gamma/3}|0\rangle_{jj}\langle r|$, $L_j^1 = \sqrt{\gamma/3}|1\rangle_{jj}\langle r|$ and

$L_j^2 = \sqrt{\gamma/3}|2\rangle_{jj}\langle r|$. Then the form of the full master equation is similar to that of Eq. (11) with the new range of $k = 0, 1, 2$. Utilizing the URP, we can derive the effective Hamiltonian as

$$\begin{aligned} H_{\rm eff} &= H_{\rm eff}^{R} + H_{\rm eff}^{MW}, \\ H_{\rm eff}^{R} &= \Omega_2(|10\rangle\langle r0| + |01\rangle\langle 0r| + |12\rangle\langle r2| + |21\rangle\langle 2r|) \\ &\quad + \text{H.c.}, \\ H_{\rm eff}^{MW} &= \omega_1(|11\rangle + |00\rangle)(\langle 01| + \langle 10|) + \omega_1(|02\rangle\langle 12| \\ &\quad + |20\rangle\langle 21|) + \omega_2(|11\rangle + |22\rangle)(\langle 21| + \langle 12|) \\ &\quad + \omega_2(|10\rangle\langle 20| + |01\rangle\langle 02|) + \text{H.c.} \\ &\quad + \delta(|00\rangle\langle 00| + |11\rangle\langle 11| + |22\rangle\langle 22| + |10\rangle\langle 10| \\ &\quad + |01\rangle\langle 01| + 2|12\rangle\langle 12| + 2|02\rangle\langle 02|). \end{aligned} \tag{15}$$

The effective master equation with the corresponding Lindblad operators can be obtained as

$$\begin{aligned} \dot{\rho} &= -i[H_{\rm eff}, \rho] + \mathcal{L}_{\rm eff}\rho, \\ \mathcal{L}_{\rm eff}\rho &= \sum_{k=1}^{6} L_{\rm eff}^{k}\rho L_{\rm eff}^{k\dagger} - \frac{1}{2}\left(L_{\rm eff}^{k\dagger}L_{\rm eff}^{k}\rho + \rho L_{\rm eff}^{k\dagger}L_{\rm eff}^{k}\right), \end{aligned} \tag{16}$$

and

$$\begin{aligned} L_{\rm eff}^{1} &= \sqrt{\frac{\gamma}{3}}|00\rangle\langle 0r|, \quad L_{\rm eff}^{2} = \sqrt{\frac{\gamma}{3}}|01\rangle\langle 0r|, \\ L_{\rm eff}^{3} &= \sqrt{\frac{\gamma}{3}}|02\rangle\langle 0r|, \quad L_{\rm eff}^{4} = \sqrt{\frac{\gamma}{3}}|00\rangle\langle r0|, \\ L_{\rm eff}^{5} &= \sqrt{\frac{\gamma}{3}}|10\rangle\langle r0|, \quad L_{\rm eff}^{6} = \sqrt{\frac{\gamma}{3}}|20\rangle\langle r0|. \end{aligned}$$

According to Eq. (16), we can notice that the ground states $\{|00\rangle, |11\rangle, |22\rangle, |01\rangle, |10\rangle, |02\rangle, |20\rangle, |12\rangle, |21\rangle\}$ are coupled with each other by the microwave fields, among which $\{|01\rangle, |10\rangle, |12\rangle, |21\rangle\}$ can be pumped into the excited states $\{|0r\rangle, |r0\rangle, |r2\rangle, |2r\rangle\}$ by the laser fields. And these excited states will further decay to ground states via atomic spontaneous emission. Hence the system will repeat the processes of pumping and decaying. However, in the absence of δ, there are two steady states in the system, $|T_1\rangle$ and $|T_2\rangle = (3|20\rangle + 3|02\rangle - 2|11\rangle - |00\rangle - |22\rangle)/2\sqrt{6}$. So we introduce δ to filter the state $|T_2\rangle$ and turn the target state $|T_1\rangle$ into the unique steady state of the system, which means the system will be stabilized at $|T_1\rangle$ without a specific initial state.

In Fig. 9, the validity of the reduced system has been verified due to the uniform behavior of evolutions of the fidelity respectively governed by the full (solid line) and effective (empty circles) master equation. It is significant that the evolution of the fidelity of $|T_1\rangle$ reaches 98.8% at $t = 8000/\Omega_1$ with a random initial state. The inset shows the fidelities of the bare states, where the fidelities of states $|00\rangle$ (solid line), $|11\rangle$ (dotted line), and $|22\rangle$ (dash-dotted line) can all reach 0.572 (the ideal values denoted by dashed line are $1/\sqrt{3} \simeq 0.577$). Then, we also investigate the feasibility to realize it experimentally. The experimental parameters are set as $(\Omega_1, \gamma) = 2\pi \times (1, 0.03)$ MHz, $\Omega_2 = 0.02\Omega_1$, $\omega_{1(2)} = 0.01\Omega_1$, and $\Delta = 100\Omega_1$. The corresponding fidelity of the target state can be above 99.14%. All the above results exhibit the reliability of the scheme for three-dimensional entanglement.

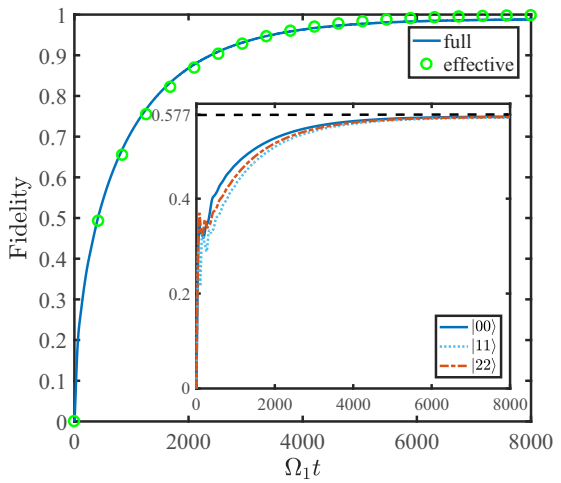

FIG. 9. The evolutions of fidelity of the three-dimensional state governed by the full (solid line) and effective master equation (empty circles). The inset shows the fidelities of the bare states. The initial states are randomly chosen as $\rho_0 = 0.15|10\rangle\langle 10| + 0.35|21\rangle\langle 21| + 0.3|01\rangle\langle 01| + 0.2|12\rangle\langle 12|$. The relevant parameters are chosen as $\Omega_2 = 0.02\Omega_1$, $\omega_{1(2)} = 0.01\Omega_1$, $\Delta = 100\Omega_1$, and $\gamma = 0.05\Omega_1$.

V. AUTONOMOUS QUANTUM ERROR CORRECTION

Quantum error correction has played an important role in the operation of quantum information processing, which is useful to protect the quantum computations from the quantum errors arising from uncontrolled interactions between the physical qubits and their environment [52–54]. Subsequently, the ingenious union of the quantum error correction and quantum dissipation was put forward by considerable ideas in theory and experiment [55–64]. Most recently, Reiter *et al.* presented an autonomous quantum error correction scheme with trapped ions [64], which inspired us to extend the URP to produce an autonomous quantum error correction scheme with dissipation.

A logical qubit encoded in three physical qubits has a general form $|\psi\rangle = \alpha|0\rangle_L + \beta|1\rangle_L = \alpha|000\rangle_P + \beta|111\rangle_P$ with $|\alpha|^2 + |\beta|^2 = 1$, where the subscripts L and P denote logical and physical, respectively. The states $|0\rangle_L$ and $|1\rangle_L$ are the basis states for the code space. We can exploit the quantum error correction to protect the qubit $|\psi\rangle$ from being converted to the single-error state $|\psi_j\rangle = \sigma_x^j|\psi\rangle$, where $\sigma_x^j = |0\rangle_{jj}\langle 1| + |1\rangle_{jj}\langle 0|$ is the bit-flip error on the jth physical qubit. The bit-flip noise can be described by $L_x^j = \sqrt{\Gamma}\sigma_x^j$, $j = 1, 2, 3$ with the bit-flip rate Γ. The corresponding master equation can reflect the noisy dynamics,

$$\begin{aligned} \dot{\rho} &= \mathcal{L}_{\rm noise}\rho \\ &= \sum_{j=1}^{3} L_x^j\rho L_x^{j\dagger} - \frac{1}{2}\left(L_x^{j\dagger}L_x^j\rho + \rho L_x^{j\dagger}L_x^j\right). \end{aligned} \tag{17}$$

In the following, we illustrate how to autonomously correct the bit-flip error via the URP in a Rydberg-atom-cavity

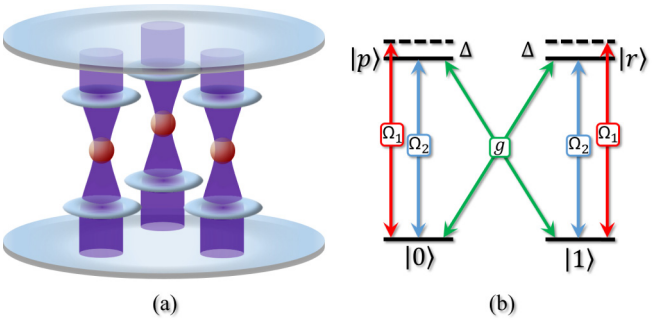

FIG. 10. (a) The setup for the autonomous quantum error correction scheme. (b) The atomic level configuration of the scheme.

system. In Fig. 10(a), we show the setup for the autonomous quantum error correction scheme, where three four-level Rydberg atoms are trapped in three independent optical cavities constructing an equilateral triangle to make the Rydberg interactions identical. The associated atomic levels are shown in Fig. 10(b), which consist of two ground states $|0\rangle$ and $|1\rangle$, and two Rydberg states $|p\rangle$ and $|r\rangle$. The ground state $|0(1)\rangle$ is used as an encoded quantum bit and is coupled with the Rydberg state $|p(r)\rangle$ by a dispersive laser field (frequency Ω_1, detuning Δ) and a resonant laser field (Rabi frequency Ω_2). Simultaneously, the transition between $|0(1)\rangle$ and $|r(p)\rangle$ is driven by the quantized cavity field resonantly with coupling strength g. In the interaction picture, the Hamiltonian reads

$$H_I = H_L + H_Q \tag{18}$$

and

$$\begin{aligned} H_L &= \sum_{j=1}^{3}(\Omega_1 e^{-i\Delta t} + \Omega_2)(|p\rangle_{jj}\langle 0| + |r\rangle_{jj}\langle 1|) + \text{H.c.} \\ &\quad + \sum_{k>j} U_{rr}^{jk}|rr\rangle_{jk}\langle rr| + U_{pp}^{jk}|pp\rangle_{jk}\langle pp| \\ &\quad + U_{rp}^{jk}|rp\rangle_{jk}\langle rp| + U_{pr}^{jk}|pr\rangle_{jk}\langle pr|, \\ H_Q &= \sum_{j=1}^{3} g(|p\rangle_{jj}\langle 1| + |r\rangle_{jj}\langle 0|)a_j + \text{H.c.}, \end{aligned}$$

where $U_{\alpha\beta}^{jk}$ stands for the Rydberg interaction between the jth atom in $|\alpha\rangle$ and the kth atom in $|\beta\rangle$, and a_j denotes the annihilation operator of the jth cavity. Once we select the suitable principal quantum numbers of Rydberg atoms [65,66], the Rydberg interactions can be considered as $U_{rr} = U_{rr}^{jk} = U_{pp}^{jk} \gg U_{rp}^{jk} = U_{pr}^{jk}$. Then we can simplify the H_L as

$$\begin{aligned} H_{\text{full}} &= \sum_{j=1}^{3}(\Omega_1 e^{-i\Delta t} + \Omega_2)(|p\rangle_{jj}\langle 0| + |r\rangle_{jj}\langle 1|) + \text{H.c.} \\ &\quad + \sum_{k>j} U_{rr}(|rr\rangle_{jk}\langle rr| + |pp\rangle_{jk}\langle pp|). \end{aligned} \tag{19}$$

The dissipative process of the jth cavity can be described as $L_c^j = \sqrt{\kappa}a_j$, where κ is the decay rate of the cavity. When we consider $\kappa \gg g$ to adiabatically eliminate a_j [67], the interaction between the jth quantized cavity field and atom

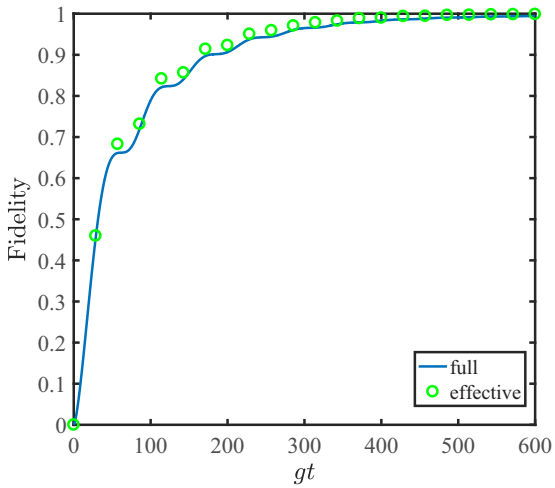

FIG. 11. The fidelity of state $(|000\rangle + i|111\rangle)/\sqrt{2}$ as a function of gt with Eq. (20) (solid line) and Eq. (21) (empty circles). The initial state is chosen as $a|\psi_1\rangle\langle\psi_1| + b|\psi_2\rangle\langle\psi_2| + c|\psi_3\rangle\langle\psi_3|$, where $|\psi_1\rangle = (|100\rangle + i|011\rangle)/\sqrt{2}$, $|\psi_2\rangle = (|010\rangle + i|101\rangle)/\sqrt{2}$, $|\psi_3\rangle = (|001\rangle + i|110\rangle)/\sqrt{2}$, $a = 0.5$, $b = 0.2$, and $c = 0.3$. The other parameters are $\Omega_1 = 3g$, $\Omega_2 = 0.05g$, $U_{rr} = \Delta = 800g$, and $\kappa_e = 0.02g$.

can be equivalent to a Lindblad operator $L_e^j = \sqrt{\kappa_e}(|0\rangle_{jj}\langle r| + |1\rangle_{jj}\langle p|)$, where $\kappa_e = 4g^2/\kappa$. The dynamics of the three-atom system can be described by a master equation

$$\begin{aligned} \dot{\rho} &= -i[H_{\text{full}}, \rho] + \mathcal{L}_e\rho, \\ \mathcal{L}_e\rho &= \sum_{j=1}^{3} L_e^j \rho L_e^{j\dagger} - \frac{1}{2}\left(L_e^{j\dagger}L_e^j\rho + \rho L_e^{j\dagger}L_e^j\right). \end{aligned} \tag{20}$$

In the condition of URP, $U_{rr} = \Delta \gg \Omega_1 \gg \Omega_2$, the evolution of the reduced system will be governed by

$$\begin{aligned} \dot{\rho} &= -i[H_{\text{eff}}, \rho] + \mathcal{L}_e\rho, \\ H_{\text{eff}} &= \Omega_2(|100\rangle\langle r00| + |010\rangle\langle 0r0| + |001\rangle\langle 00r| \\ &\quad + |110\rangle\langle 00p| + |101\rangle\langle 0p0| + |011\rangle\langle p00|) \\ &\quad + \text{H.c.} \end{aligned} \tag{21}$$

One can find that our scheme can correct the single-error states by pumping them to the single excited states, which further decay to the desired stable states $|000\rangle$ or $|111\rangle$ via leaky cavities. In order to visually reveal the correcting process, we study how the three-atom system evolves when the bit-flip noise makes the state $(|000\rangle + i|111\rangle)/\sqrt{2}$ into a single-error mixed state, $a|\psi_1\rangle\langle\psi_1| + b|\psi_2\rangle\langle\psi_2| + c|\psi_3\rangle\langle\psi_3|$, where $|\psi_1\rangle = (|100\rangle + i|011\rangle)/\sqrt{2}$, $|\psi_2\rangle = (|010\rangle + i|101\rangle)/\sqrt{2}$, and $|\psi_3\rangle = (|001\rangle + i|110\rangle)/\sqrt{2}$. We show the fidelity of the state $(|000\rangle + i|111\rangle)/\sqrt{2}$ as a function of gt with Eq. (20) (solid line) and Eq. (21) (empty circles) in Fig. 11. The initial state is the single-error mixed state $a|\psi_1\rangle\langle\psi_1| + b|\psi_2\rangle\langle\psi_2| + c|\psi_3\rangle\langle\psi_3|$, and we choose $a = 0.5$, $b = 0.2$, and $c = 0.3$ in the numerical simulation. It is clear enough that the two curves are in good agreement with each other and a high fidelity of up to 99.6% at $gt = 1000$ can

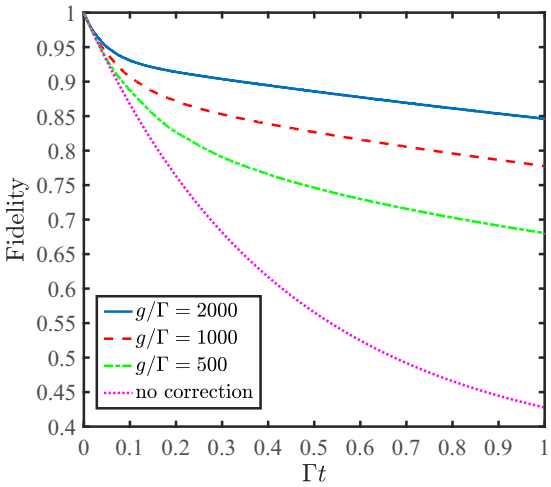

FIG. 12. The evolution of the fidelity of state $(|000\rangle + i|111\rangle)/\sqrt{2}$ governed by the Eq. (22) with different coupling strengths g. The initial state is $|\psi(0)\rangle = (|000\rangle + i|111\rangle)/\sqrt{2}$, and the relevant parameters are $\Omega_1 = 3g$, $\Omega_2 = 0.05g$, $U_{rr} = \Delta = 800g$, and $\kappa_e = 0.02g$.

be obtained. The appearance affirms the feasibility of our quantum error correction scheme and the correctness of the reduced system. In experiment, the transition $|0\rangle \leftrightarrow |r\rangle$ requires two indirect transitions to realize [12,68,69]. First, the ground state $|0\rangle$ is dispersively coupled with an intermediate state $|e\rangle$ by an optical cavity with strength g_b, detuning $-\Delta_b$. Second, the intermediate state $|e\rangle$ will be pumped to the Rydberg state $|r\rangle$ via a classical field with Rabi frequency Ω_b, detuning Δ_b. In the regime of the large detuning, $|\Delta_b| \gg \{g_b, \Omega_b\}$, the intermediate state $|e\rangle$ can be eliminated adiabatically and an equivalent direct transition $|0\rangle \leftrightarrow |r\rangle$ can be accomplished with an effective strength $g_{\text{eff}} = g_b\Omega_b/\Delta_b$, which is analogous to the strength g in our scheme. Consequently, we can experimentally regulate the value of Δ_b to obtain desired values of g and κ_e. Then we substitute a group of experimental parameters $(\Omega_1, \Omega_2, \Delta, \gamma, \kappa_e) = 2\pi \times (3, 0.05, 800, 0.001, 0.02)$ MHz and the fidelity of state $(|000\rangle + i|111\rangle)/\sqrt{2}$ can be above 97.34%.

In Fig. 12, we analyze the capability of autonomously correcting the single-error state as the bit-flip noise continuously emerges. The total process of autonomous quantum error correction reads

$$\dot{\rho} = -i[H_{\text{full}}, \rho] + \mathcal{L}_e\rho + \mathcal{L}_{\text{noise}}\rho. \tag{22}$$

When the error correction is absent (dotted line), the fidelity will steeply descend to 42.77% at $\Gamma t = 1$. Nevertheless, as long as the error correction arises, the bit-flip noise can be autonomously and continuously corrected, and the decline of fidelity will be repressed remarkably with the enhancement of g. At $\Gamma t = 1$, the fidelity can reach 68.05%, 77.77%, and 84.62% with $g = 500\Gamma$ (dash-dotted line), $g = 1000\Gamma$ (dashed line), and $g = 2000\Gamma$ (solid line), respectively.

VI. SUMMARY

In summary, we have successfully realized an unconventional Rydberg pumping (URP) mechanism via the organic combination of Rydberg interaction and two classical fields. We can take advantage of the URP to freeze the evolution of the states with two atoms at the same ground state and excite the states with two atoms at different ground states. Then we apply the URP to actualize the three-qubit controlled-PHASE gate, the two- and three-dimensional steady-state entanglement, and the autonomous quantum error correction. The corresponding results can adequately evidence the feasibility of all the above applications by considering the state-of-the-art technology. We believe our scheme supplies a new prospect with regard to quantum information processing with neutral atoms.

ACKNOWLEDGMENT

This work is supported by National Natural Science Foundation of China (NSFC) under Grant No. 11774047.

[1] M. Saffman, T. G. Walker, and K. Mølmer, Quantum information with Rydberg atoms, Rev. Mod. Phys. **82**, 2313 (2010).
[2] D. Jaksch, J. I. Cirac, P. Zoller, S. L. Rolston, R. Côté, and M. D. Lukin, Fast Quantum Gates for Neutral Atoms, Phys. Rev. Lett. **85**, 2208 (2000).
[3] D. Møller, L. B. Madsen, and K. Mølmer, Quantum Gates and Multiparticle Entanglement by Rydberg Excitation Blockade and Adiabatic Passage, Phys. Rev. Lett. **100**, 170504 (2008).
[4] L. Isenhower, E. Urban, X. L. Zhang, A. T. Gill, T. Henage, T. A. Johnson, T. G. Walker, and M. Saffman, Demonstration of a Neutral Atom Controlled-NOT Quantum Gate, Phys. Rev. Lett. **104**, 010503 (2010).
[5] D. Barredo, S. Ravets, H. Labuhn, L. Béguin, A. Vernier, F. Nogrette, T. Lahaye, and A. Browaeys, Demonstration of a Strong Rydberg Blockade in Three-Atom Systems with Anisotropic Interactions, Phys. Rev. Lett. **112**, 183002 (2014).
[6] D. Petrosyan and K. Mølmer, Binding Potentials and Interaction Gates Between Microwave-Dressed Rydberg Atoms, Phys. Rev. Lett. **113**, 123003 (2014).
[7] D. D. B. Rao and K. Mølmer, Robust Rydberg-interaction gates with adiabatic passage, Phys. Rev. A **89**, 030301(R) (2014).
[8] X.-F. Shi, Rydberg Quantum Gates Free from Blockade Error, Phys. Rev. Appl. **7**, 064017 (2017).
[9] X.-F. Shi, Deutsch, Toffoli, and CNOT Gates via Rydberg Blockade of Neutral Atoms, Phys. Rev. Appl. **9**, 051001 (2018).
[10] M. Saffman and K. Mølmer, Efficient Multiparticle Entanglement via Asymmetric Rydberg Blockade, Phys. Rev. Lett. **102**, 240502 (2009).
[11] X. L. Zhang, L. Isenhower, A. T. Gill, T. G. Walker, and M. Saffman, Deterministic entanglement of two neutral atoms via Rydberg blockade, Phys. Rev. A **82**, 030306 (2010).

[12] T. Wilk, A. Gaëtan, C. Evellin, J. Wolters, Y. Miroshnychenko, P. Grangier, and A. Browaeys, Entanglement of Two Individual Neutral Atoms Using Rydberg Blockade, Phys. Rev. Lett. **104**, 010502 (2010).

[13] D. D. B. Rao and K. Mølmer, Dark Entangled Steady States of Interacting Rydberg Atoms, Phys. Rev. Lett. **111**, 033606 (2013).

[14] S. Möbius, M. Genkin, A. Eisfeld, S. Wüster, and J. M. Rost, Entangling distant atom clouds through Rydberg dressing, Phys. Rev. A **87**, 051602 (2013).

[15] I. I. Beterov, G. N. Hamzina, E. A. Yakshina, D. B. Tretyakov, V. M. Entin, and I. I. Ryabtsev, Adiabatic passage of radio-frequency-assisted Förster resonances in Rydberg atoms for two-qubit gates and the generation of Bell states, Phys. Rev. A **97**, 032701 (2018).

[16] A.-X. Chen, Implementation of Deutsch-Jozsa algorithm and determination of value of function via Rydberg blockade, Opt. Exp. **19**, 2037 (2011).

[17] H. Weimer, M. Muller, I. Lesanovsky, P. Zoller, and H. P. Buchler, A Rydberg quantum simulator, Nat. Phys. **6**, 382 (2010).

[18] Y. Han, B. He, K. Heshami, C.-Z. Li, and C. Simon, Quantum repeaters based on Rydberg-blockade-coupled atomic ensembles, Phys. Rev. A **81**, 052311 (2010).

[19] I. Bouchoule and K. Mølmer, Spin squeezing of atoms by the dipole interaction in virtually excited Rydberg states, Phys. Rev. A **65**, 041803 (2002).

[20] J. E. Johnson and S. L. Rolston, Interactions between Rydberg-dressed atoms, Phys. Rev. A **82**, 033412 (2010).

[21] J. B. Balewski, A. T. Krupp, A. Gaj, S. Hofferberth, R. Löw, and T. Pfau, Rydberg dressing: Understanding of collective many-body effects and implications for experiments, New J. Phys. **16**, 063012 (2014).

[22] G. Pupillo, A. Micheli, M. Boninsegni, I. Lesanovsky, and P. Zoller, Strongly Correlated Gases of Rydberg-Dressed Atoms: Quantum and Classical Dynamics, Phys. Rev. Lett. **104**, 223002 (2010).

[23] S. Yan, D. A. Huse, and S. R. White, Spin-liquid ground state of the s $= 1/2$ kagome Heisenberg antiferromagnet, Science **332**, 1173 (2011).

[24] N. Henkel, F. Cinti, P. Jain, G. Pupillo, and T. Pohl, Supersolid Vortex Crystals in Rydberg-Dressed Bose-Einstein Condensates, Phys. Rev. Lett. **108**, 265301 (2012).

[25] P. Mason, C. Josserand, and S. Rica, Activated Nucleation of Vortices in a Dipole-Blockaded Supersolid Condensate, Phys. Rev. Lett. **109**, 045301 (2012).

[26] Y.-Y. Jau, A. M. Hankin, T. Keating, I. H. Deutsch, and G. W. Biedermann, Entangling atomic spins with a Rydberg-dressed spin-flip blockade, Nat. Phys. **12**, 71 (2016).

[27] C. Ates, T. Pohl, T. Pattard, and J. M. Rost, Antiblockade in Rydberg Excitation of an Ultracold Lattice Gas, Phys. Rev. Lett. **98**, 023002 (2007).

[28] T. Amthor, C. Giese, C. S. Hofmann, and M. Weidemüller, Evidence of Antiblockade in an Ultracold Rydberg Gas, Phys. Rev. Lett. **104**, 013001 (2010).

[29] S.-L. Su, E. Liang, S. Zhang, J.-J. Wen, L.-L. Sun, Z. Jin, and A.-D. Zhu, One-step implementation of the Rydberg-Rydberg-interaction gate, Phys. Rev. A **93**, 012306 (2016).

[30] S.-L. Su, Y. Gao, E. Liang, and S. Zhang, Fast Rydberg antiblockade regime and its applications in quantum logic gates, Phys. Rev. A **95**, 022319 (2017).

[31] S. L. Su, H. Z. Shen, Erjun Liang, and S. Zhang, One-step construction of the multiple-qubit Rydberg controlled-PHASE gate, Phys. Rev. A **98**, 032306 (2018).

[32] A. W. Carr and M. Saffman, Preparation of Entangled and Antiferromagnetic States by Dissipative Rydberg Pumping, Phys. Rev. Lett. **111**, 033607 (2013).

[33] S.-L. Su, Q. Guo, H.-F. Wang, and S. Zhang, Simplified scheme for entanglement preparation with Rydberg pumping via dissipation, Phys. Rev. A **92**, 022328 (2015).

[34] S.-L. Su, Y. Tian, H. Z. Shen, H. Zang, E. Liang, and S. Zhang, Applications of the modified Rydberg antiblockade regime with simultaneous driving, Phys. Rev. A **96**, 042335 (2017).

[35] J. Song, C. Li, Z.-J. Zhang, Y.-Y. Jiang, and Y. Xia, Implementing stabilizer codes in noisy environments, Phys. Rev. A **96**, 032336 (2017).

[36] X. Q. Shao, J. H. Wu, X. X. Yi, and Gui-Lu Long, Dissipative preparation of steady Greenberger-Horne-Zeilinger states for Rydberg atoms with quantum zeno dynamics, Phys. Rev. A **96**, 062315 (2017).

[37] D.-X. Li, X.-Q. Shao, J.-H. Wu, and X. X. Yi, Dissipation-induced w state in a Rydberg-atom-cavity system, Opt. Lett. **43**, 1639 (2018).

[38] X. Q. Shao, D. X. Li, Y. Q. Ji, J. H. Wu, and X. X. Yi, Ground-state blockade of Rydberg atoms and application in entanglement generation, Phys. Rev. A **96**, 012328 (2017).

[39] P. W. Shor, *Proceedings of the 35th Annual Symposium on Foundations of Computer Science* (IEEE Computer Society, Los Alamitos, CA, 1994).

[40] L. K. Grover, Quantum Mechanics Helps in Searching for a Needle in a Haystack, Phys. Rev. Lett. **79**, 325 (1997).

[41] L. K. Grover, Quantum Computers can Search Arbitrarily Large Databases by a Single Query, Phys. Rev. Lett. **79**, 4709 (1997).

[42] M. A. Nilsen and I. L. Chuang, *Quantum Computation and Quantum Information* (Cambridge University Press, Cambridge, UK, 2000).

[43] J. Qian, G. Dong, L. Zhou, and W. Zhang, Phase diagram of Rydberg atoms in a nonequilibrium optical lattice, Phys. Rev. A **85**, 065401 (2012).

[44] X.-F. Zhang, Q. Sun, Y.-C. Wen, W.-M. Liu, S. Eggert, and A.-C. Ji, Rydberg Polaritons in a Cavity: A Superradiant Solid, Phys. Rev. Lett. **110**, 090402 (2013).

[45] M. J. Kastoryano, F. Reiter, and A. S. Sørensen, Dissipative Preparation of Entanglement in Optical Cavities, Phys. Rev. Lett. **106**, 090502 (2011).

[46] X.-Q. Shao, T.-Y. Zheng, C. H. Oh, and S. Zhang, Dissipative Creation of Three-Dimensional Entangled State in Optical Cavity Via Spontaneous Emission, Phys. Rev. A **89**, 012319 (2014).

[47] F. Reiter, D. Reeb, and A. S. Sørensen, Scalable Dissipative Preparation of Many-Body Entanglement, Phys. Rev. Lett. **117**, 040501 (2016).

[48] A. Grankin, E. Brion, E. Bimbard, R. Boddeda, I. Usmani, A. Ourjoumtsev, and P. Grangier, Quantum Statistics of Light Transmitted Through an Intracavity Rydberg Medium, New J. Phys. **16**, 043020 (2014).

[49] D. Kaszlikowski, P. Gnaciński, M. Zukowski, W. Miklaszewski, and A. Zeilinger, Violations of Local Realism by Two

Entangled N-Dimensional Systems are Stronger than for Two Qubits, Phys. Rev. Lett. **85**, 4418 (2000).

[50] T. Durt, N. J. Cerf, N. Gisin, and M. Zukowski, Security of quantum key distribution with entangled qutrits, Phys. Rev. A **67**, 012311 (2003).

[51] T. Durt, D. Kaszlikowski, J.-L. Chen, and L. C. Kwek, Security of quantum key distributions with entangled qudits, Phys. Rev. A **69**, 032313 (2004).

[52] P. W. Shor, Scheme for reducing decoherence in quantum computer memory, Phys. Rev. A **52**, R2493 (1995).

[53] A. M. Steane, Error Correcting Codes in Quantum Theory, Phys. Rev. Lett. **77**, 793 (1996).

[54] D. P. DiVincenzo and P. W. Shor, Fault-Tolerant Error Correction with Efficient Quantum Codes, Phys. Rev. Lett. **77**, 3260 (1996).

[55] J. P. Paz and W. H. Zurek, Continuous error correction, Proc. R. Soc. London, Ser. A **454**, 355 (1998).

[56] C. Ahn, A. C. Doherty, and A. J. Landahl, Continuous quantum error correction via quantum feedback control, Phys. Rev. A **65**, 042301 (2002).

[57] K. Fujii, M. Negoro, N. Imoto, and M. Kitagawa, Measurement-Free Topological Protection Using Dissipative Feedback, Phys. Rev. X **4**, 041039 (2014).

[58] Z. Leghtas, S. Touzard, I. M. Pop, A. Kou, B. Vlastakis, A. Petrenko, K. M. Sliwa, A. Narla, S. Shankar, M. J. Hatridge, M. Reagor, L. Frunzio, R. J. Schoelkopf, M. Mirrahimi, and M. H. Devoret, Confining the state of light to a quantum manifold by engineered two-photon loss, Science **347**, 853 (2015).

[59] M. Ippoliti, L. Mazza, M. Rizzi, and V. Giovannetti, Perturbative approach to continuous-time quantum error correction, Phys. Rev. A **91**, 042322 (2015).

[60] E. Kapit, J. T. Chalker, and S. H. Simon, Passive correction of quantum logical errors in a driven, dissipative system: A blueprint for an analog quantum code fabric, Phys. Rev. A **91**, 062324 (2015).

[61] E. Kapit, Hardware-Efficient and Fully Autonomous Quantum Error Correction in Superconducting Circuits, Phys. Rev. Lett. **116**, 150501 (2016).

[62] C. D. Freeman, C. M. Herdman, and K. B. Whaley, Engineering autonomous error correction in stabilizer codes at finite temperature, Phys. Rev. A **96**, 012311 (2017).

[63] C. Shen, K. Noh, V. V. Albert, S. Krastanov, M. H. Devoret, R. J. Schoelkopf, S. M. Girvin, and L. Jiang, Quantum channel construction with circuit quantum electrodynamics, Phys. Rev. B **95**, 134501 (2017).

[64] F. Reiter, A. S. Sørensen, P. Zoller, and C. A. Muschik, Dissipative quantum error correction and application to quantum sensing with trapped ions, Nat. Commun. **8**, 1822 (2017).

[65] T. G. Walker and M. Saffman, Consequences of Zeeman degeneracy for the Van der Waals blockade between Rydberg atoms, Phys. Rev. A **77**, 032723 (2008).

[66] Y.-M. Liu, X.-D. Tian, D. Yan, Y. Zhang, C.-L. Cui, and J.-H. Wu, Nonlinear modifications of photon correlations via controlled single and double Rydberg blockade, Phys. Rev. A **91**, 043802 (2015).

[67] F. Reiter and A. S. Sørensen, Effective operator formalism for open quantum systems, Phys. Rev. A **85**, 032111 (2012).

[68] A. Gaëtan, Y. Miroshnychenko, T. Wilk, A. Chotia, M. Viteau, D. Comparat, P. Pillet, A. Browaeys, and P. Grangier, Observation of collective excitation of two individual atoms in the Rydberg blockade regime, Nat. Phys. **5**, 115 (2009).

[69] X. Q. Shao, J. H. Wu, and X. X. Yi, Dissipative stabilization of quantum-feedback-based multipartite entanglement with Rydberg atoms, Phys. Rev. A **95**, 022317 (2017).